Journal of Zhejiang University-SCIENCE C (Computers & Electronics)
ISSN 1869-1951 (Print); ISSN 1869-196X (Online)
www.zju.edu.cn/jzus; www.springerlink.com
E-mail: jzus@zju.edu.cn

Robust synchronization of chaotic systems using sliding mode and feedback control*

Li-li LI[1], Ying LIU‡[2], Qi-guo YAO[1]

([1]*School of Naval Architecture and Ocean Engineering, Zhejiang Ocean University, Zhoushan 316000, China*)

([2]*Department of Information Science and Electronic Engineering, Zhejiang University, Hangzhou 310027, China*)

E-mail: 64452300@qq.com; yingliu@zju.edu.cn; yaoqiguo@163.com

Received Sept. 21, 2013; Revision accepted Dec. 13, 2013; Crosschecked Feb. 19, 2014

Abstract: We propose a robust scheme to achieve the synchronization of chaotic systems with modeling mismatches and parametric variations. The proposed algorithm combines high-order sliding mode and feedback control. The sliding mode is used to estimate the synchronization error between the master and the slave as well as its time derivatives, while feedback control is used to drive the slave track the master. The stability of the proposed design is proved theoretically, and its performance is verified by some numerical simulations. Compared with some existing synchronization algorithms, the proposed algorithm shows faster convergence and stronger robustness to system uncertainties.

Key words: Chaos synchronization, Sliding mode, Feedback control
doi:10.1631/jzus.C1300266 **Document code:** A **CLC number:** TP273

1 Introduction

Since the pioneering work of Pecora and Carroll (1990), chaos synchronization has become an attracting research topic in nonlinear science, and has been widely used in many applications, such as secure communications (Kocarev and Parlitz, 1995; Femat *et al.*, 2001; Feki, 2003), animal gaits (Collins and Stewart, 1993), and biological oscillators (Wittmeier *et al.*, 2008; Mao *et al.*, 2009). Consequently, various synchronization schemes have been proposed, such as drive-response synchronization (Pecora and Carroll, 1991), master-slave synchronization (Kocarev and Parlitz, 1995), observer-based synchronization (Nijmeijer and Ymareels, 1997; Grassi and Mascoio, 1999), adaptive synchronization (Besancon, 2000; Yu and Parlitz, 2008; Liu *et al.*, 2008; Liu and Tang, 2009), and geometrical control (Freitas *et al.*, 2005; Chen and Kurths, 2007).

In some practical situations, system uncertainties, such as parameter mismatches and structural differences, unavoidably exist in nature, and hence the structures of the master and the slave are not exactly the same. For instance, biological oscillators are found to be synchronous even if the considered two oscillators have different dynamics (Collins and Stewart, 1993). The model mismatches between the master and the slave make the real control problem much more complicated. Therefore, it is more desirable if a robust strategy can be designed such that the synchronization between two chaotic systems can be established.

To tackle this problem, many robust synchronization schemes have been proposed in the literature (Karimi and Gao, 2010; Karimi, 2011; Trentelman *et al.*, 2013; Youssef *et al.*, 2013). H_∞ theory based on Lyapunov stability theory and linear matrix inequality formulation is an efficient approach

‡ Corresponding author

* Project supported by the National Natural Science Foundation of China (No. 61101045), the Natural Science Foundation of Zhejiang Province of China (No. LY13E090004), and the Department of Graduate of Zhejiang Ocean University (No. 20(2012))

©Zhejiang University and Springer-Verlag Berlin Heidelberg 2014

to handle such problems, which has been studied in Karimi and Gao (2010) and Karimi (2011) and the references therein. However, these synchronization methods are usually specialized for a particular chaotic system, and thus may not be applicable to other chaotic systems. Considering this, Wang *et al.* (2012) developed a systematic H_∞ robust synchronization approach for a class of chaotic systems that can be transformed into the canonical form through some topological transformation, such as the Chen system, Lorenz system, Duffing oscillators, and Hindmarsh-Rose neuronal model. To ensure global convergence, this strategy requires that the information of all the state variables should be available. However, this condition may not be satisfied in practice due to the limitation in measuring conditions. On the other hand, by lumping the system uncertainties into a new state variable, an extended state observer (ESO) (Han, 1995) together with a systematic robust asymptotic continuous feedback's controller has been proposed in Femat *et al.* (1999) and Femat and Solis-Perales (2008). This method does not require any priori information about the system model, and only one state variable is required to design the controller, which makes the complex control problem physically realizable. Yet, to achieve the acceptable performance of synchronization, a long time is needed.

In addition to the aforementioned robust strategies, the sliding mode method, which is insensitive to system parameters or perturbations, is another kind of robust synchronization strategy. Recently, sliding mode based synchronization strategies have aroused considerable interest and been widely used in synchronization of complex high-order nonlinear dynamic systems with some uncertainties, see Yang and Shao (2002), Bowong (2004), Li *et al.* (2005), and Karimi (2012) to name a few. However, the performances of these methods are highly dependent on the parameters for constructing the control surface. If the design parameters are improper, the performance of synchronization may become quite poor. To reduce the sensitivity to the parameters, a robust differentiator estimator using a quasi-continuous high-order sliding mode has been proposed in Levant (2003), Levant and Pavlov (2008), and Rodríguez *et al.* (2008) such that the finite-time synchronization between two non-identical systems can be achieved. Unfortunately, this design is of high computation cost and thus the time for reaching synchronization is intolerably long. So, it is computationally inefficient if the order of the sliding mode is higher, which hampers its application to high-dimensional systems and complex networks.

Considering this, in this paper, a synthesis of high-order sliding mode and feedback control based on ESO is proposed such that the advantages of these two methods can be fully exploited. In the proposed approach, the high-order sliding mode is used to obtain the estimates for the output error and its time derivatives, while the linearizing feedback control is designed to drive the slave to follow the master. In this way, the synchronization time as well as the computational complexity can be reduced. The stability of the proposed design is proved mathematically, while its performance is verified numerically by simulations.

2 Synchronization of chaotic systems with uncertainties

2.1 Problem statement

Consider a master nonlinear system as follows:

$$\begin{cases} \dot{\boldsymbol{x}}_{\mathrm{m}} = f(\boldsymbol{x}_{\mathrm{m}}, \boldsymbol{p}), \\ \boldsymbol{y}_{\mathrm{m}} = h(\boldsymbol{x}_{\mathrm{m}}) = \boldsymbol{C}_{\mathrm{m}}\boldsymbol{x}_{\mathrm{m}}, \end{cases} \tag{1}$$

where $\boldsymbol{x}_{\mathrm{m}} \in \mathbb{R}^n$ denotes the state vector, $f : \mathbb{R}^n \to \mathbb{R}^n$ is a smooth function, $\boldsymbol{p}$ is the parametric vector, $\boldsymbol{y}_{\mathrm{m}}$ is the system output (measurable state), and $h(\boldsymbol{x}_{\mathrm{m}}) = \boldsymbol{C}_{\mathrm{m}}\boldsymbol{x}_{\mathrm{m}}$ is the output of the master with $\boldsymbol{C}_{\mathrm{m}}$ being a constant vector.

Let us now take a slave system with the same order as system (1):

$$\begin{cases} \dot{\boldsymbol{x}}_{\mathrm{s}} = f(\boldsymbol{x}_{\mathrm{s}}, \boldsymbol{q}) + g(\boldsymbol{x}_{\mathrm{s}})u, \\ \boldsymbol{y}_{\mathrm{s}} = h(\boldsymbol{x}_{\mathrm{s}}) = \boldsymbol{C}_{\mathrm{s}}\boldsymbol{x}_{\mathrm{s}}, \end{cases} \tag{2}$$

where $\boldsymbol{x}_{\mathrm{s}} \in \mathbb{R}^n$ denotes the state vector of system (2), $g(\boldsymbol{x}_{\mathrm{s}})$ is a vector depending on $\boldsymbol{x}_{\mathrm{s}}$, $u \in \mathbb{R}$ is a control signal, $\boldsymbol{q}$ is the parametric vector, and $\boldsymbol{p} \neq \boldsymbol{q}$. $\boldsymbol{C}_{\mathrm{s}}$ defines the measured state of the slave system, and $h(\boldsymbol{x}_{\mathrm{s}}) = \boldsymbol{C}_{\mathrm{s}}\boldsymbol{x}_{\mathrm{s}}$ defines the output of the slave. Here, we assume that $\boldsymbol{C}_{\mathrm{m}} = \boldsymbol{C}_{\mathrm{s}}$. Note that the subscripts 'm' and 's' are used to present the master system and the slave system, respectively.

Subtracting system (1) from (2), we have the

error dynamics:

$$\begin{cases} \dot{\boldsymbol{e}} = \dot{\boldsymbol{x}}_{\mathrm{s}} - \dot{\boldsymbol{x}}_{\mathrm{m}} = \Delta f(\boldsymbol{x}_{\mathrm{m}}, \boldsymbol{x}_{\mathrm{s}}, \boldsymbol{p}, \boldsymbol{q}) + g(\boldsymbol{x}_{\mathrm{s}})u, \\ y = h(\boldsymbol{e}), \end{cases} \tag{3}$$

where $e_i = x_{i\mathrm{s}} - x_{i\mathrm{m}}$ for $i = 1, 2, \cdots, n$, $\Delta f = f(\boldsymbol{x}_{\mathrm{s}}, \boldsymbol{q}) - f(\boldsymbol{x}_{\mathrm{m}}, \boldsymbol{p})$ is a smooth vector, denoting the differences between the master and the slave, and $y = h(\boldsymbol{e})$ is a smooth function defining their output errors. Note that the synchronization between systems (1) and (2) is equivalent to the stabilization of system (3). In other words, the problem of synchronization can be reduced to the design of suitable feedback control u such that $\lim\limits_{t\to\infty} \boldsymbol{e} \to \boldsymbol{0}$, i.e., $\boldsymbol{x}_{\mathrm{s}} \to \boldsymbol{x}_{\mathrm{m}}$.

2.2 Preliminaries

To illustrate the main results of this study, some preliminaries are given first.

Theorem 1 (Isidori, 1989) Consider the following system:

$$\begin{cases} \dot{\boldsymbol{x}} = f(\boldsymbol{x}) + g(\boldsymbol{x})u, \\ \boldsymbol{y} = h(\boldsymbol{x}), \end{cases} \tag{4}$$

where $\boldsymbol{x} \in \mathbb{R}^n$ represents the state vector, $f : \mathbb{R}^n \to \mathbb{R}^n$ is a smooth function, u is a control signal, and $\boldsymbol{y}$ is the system output. It is assumed that there exists the smallest integer ρ such that the following conditions are satisfied: (1) $L_g L_f^i h(\boldsymbol{x}) = 0, i = 1, 2, \cdots, \rho - 2$; (2) $L_g L_f^{\rho-1} h(\boldsymbol{x}) \neq 0$, where $L_f^\rho h(\boldsymbol{x}) := L_f(L_f^{\rho-1} h(\boldsymbol{x}))$, $L_f^0 h(\boldsymbol{x}) := h(\boldsymbol{x})$, and $L_f h(\boldsymbol{x}) := \dfrac{\partial h(\boldsymbol{x})}{\partial \boldsymbol{x}} f(\boldsymbol{x})$ is the Lie derivative of $h(\boldsymbol{x})$ along $f(\boldsymbol{x})$. Then, it is always possible to find $(n-\rho)$ functions $\Phi_{\rho+1}, \Phi_{\rho+2}, \cdots, \Phi_n$ with $L_g \Phi_i \neq 0, i = \rho+1, \rho+2, \cdots, n$ such that system (4) can be globally transformed into the following canonical form:

$$\begin{cases} \dot{z}_i = z_{i+1}, \quad i = 1, 2, \cdots, \rho - 1, \\ \dot{z}_\rho = \alpha(\boldsymbol{z}, \boldsymbol{\zeta}) + \beta(\boldsymbol{z}, \boldsymbol{\zeta})u, \quad \beta(\boldsymbol{z}, \boldsymbol{\zeta}) \neq 0, \end{cases} \tag{5a}$$

$$\begin{cases} \dot{\boldsymbol{\zeta}} = \Psi(\boldsymbol{z}, \boldsymbol{\zeta}), \quad \boldsymbol{\zeta} \in \mathbb{R}^{n-\rho}, \\ y = z_1, \end{cases} \tag{5b}$$

where $\alpha(\boldsymbol{z}, \boldsymbol{\zeta}) = L_f^\rho h(\boldsymbol{x})$ and $\beta(\boldsymbol{z}, \boldsymbol{\zeta}) = L_g L_f^{\rho-1} h(\boldsymbol{x}) \neq 0$, are uncertain. $\Psi(\boldsymbol{z}, \boldsymbol{\zeta}) = [\Phi_{\rho+1}, \Phi_{\rho+2}, \cdots, \Phi_{\rho+n}]$ is a matrix such that the coordinate transformation $\Phi(\boldsymbol{x}) = [h(\boldsymbol{x}), L_f h(\boldsymbol{x}), \cdots, L_f^{\rho-1} h(\boldsymbol{x}), \Phi_{\rho+1}, \Phi_{\rho+2}, \cdots, \Phi_{\rho+n}]$ is globally invertible. $\dot{\boldsymbol{\zeta}} = \Psi(0, \boldsymbol{\zeta})$ is called zero dynamics of the system. Note that the system is called fully linearizable when $\rho = n$, while it is called partly linearizable when $\rho < n$.

Assumptions: Considering the dynamical system (1), the following assumptions are required (Femat *et al.*, 1999; Femat and Solis-Perales, 2008):

Assumption 1 There is only a single system state as the output. Without loss of generality, one can let $y_{\mathrm{m}} = h(\boldsymbol{x}_{\mathrm{m}}) = x_{1\mathrm{m}}$; i.e., only the first system state is measurable.

Assumption 2 There are some unknown model mismatches between the master and the slave, i.e., $\Delta f \neq 0$.

Assumption 3 The error dynamical system can be transformed into a canonical form; i.e., there exists a diffeomorphism transformation of coordinate for system (3).

Assumption 4 System (3) is a minimum-phase system.

Remark 1 It is noted that Assumption 1 is more agreeable in practice. For example, in real communications, only a scalar time series is transmitted to construct the synchronization between the master and the slave for security (Femat *et al.*, 2001; Feki, 2003), and for a biological neuronal model, due to the limitation of the measuring condition, only the membrane potential is obtainable for each neuron (Yu and Parlitz, 2008).

Remark 2 As mentioned before, the mismatches between the master and the slave unavoidably exist in nature, and hence Δf always exists.

Remark 3 It is noted that many chaotic systems can be transformed into a canonical form through a mathematical transformation. Based on Lemma 1 given in Eq. (A1) in Appendix A, the error dynamical system (3) can be changed into a canonical form as given in Eq. (5).

Remark 4 The minimum phase implies that the subsystem of the zero dynamics $\dot{\boldsymbol{\zeta}} = \Psi(0, \boldsymbol{\zeta})$ is asymptotically stable. Although this condition is strong, it can be satisfied for some chaotic systems, such as the Lorenz system and Chen system.

2.3 Design of a robust synchronization scheme

In this subsection, a new robust synchronization scheme is proposed based on a combination of high-order sliding mode and linearizing feedback control.

According to Theorem 1, by lumping the uncertainties into a new state variable, the error dynamics (3) can be further rearranged into the following canonical form:

$$\begin{cases} \dot{z}_i = z_{i+1}, \quad i = 1, 2, \cdots, \rho - 1, \\ \dot{z}_\rho = z_{\rho+1} + \beta_{\mathrm{E}}(\boldsymbol{z})u, \\ \dot{z}_{\rho+1} = \Gamma(\boldsymbol{z}, z_{\rho+1}, \boldsymbol{\zeta}, u), \end{cases} \tag{6a}$$

$$\begin{cases} \dot{\boldsymbol{\zeta}} = \Psi(\boldsymbol{z}, \boldsymbol{\zeta}), \\ y = z_1 = e_1, \end{cases} \tag{6b}$$

where $\beta_{\mathrm{E}}(\boldsymbol{z})$ is bounded, $z_{\rho+1} = \Theta(\boldsymbol{z}, \boldsymbol{\zeta}, u) = \alpha(\boldsymbol{z}, \boldsymbol{\zeta}) + \delta(\boldsymbol{z}, \boldsymbol{\zeta})u$ and $\delta(\boldsymbol{z}, \boldsymbol{\zeta}) = \beta(\boldsymbol{z}, \boldsymbol{\zeta}) - \beta_{\mathrm{E}}(\boldsymbol{z})$. $\Gamma(\boldsymbol{z}, z_{\rho+1}, \boldsymbol{\zeta}, u) = \sum_{i=1}^{\rho-1}[z_{i+1}\partial_i\Theta(\boldsymbol{z}, \boldsymbol{\zeta}, u)] + [z_{\rho+1} + \beta_{\mathrm{E}}(\boldsymbol{z})]\partial_\rho\Theta(\boldsymbol{z}, \boldsymbol{\zeta}, u) + \delta(\boldsymbol{z}, \boldsymbol{\zeta})\dot{u} + \partial_t\delta(\boldsymbol{z}, \boldsymbol{\zeta})u + \partial_{\boldsymbol{\zeta}}\Theta(\boldsymbol{z}, \boldsymbol{\zeta}, u)\Psi(\boldsymbol{z}, \boldsymbol{\zeta})$, where $\partial_i\Theta(\boldsymbol{z}, \boldsymbol{\zeta}, u) = \partial\Theta(\boldsymbol{z}, \boldsymbol{\zeta}, u)/\partial x_i, i = 1, 2, \cdots, \rho$.

From system (6), it can be seen that the mismatches between the master and the slave have been lumped into a nonlinear function $\Theta(\boldsymbol{z}, \boldsymbol{\zeta}, u)$, which can be interpreted as an augmented state variable $z_{\rho+1}$. Then, the problem of synchronization between systems (1) and (2) can be considered as the stabilization of error dynamics (6). To achieve this goal, a suitable feedback controller u must be designed. To simplify the design, a linearizing feedback controller similar to that given in Femat *et al.* (1999) and Femat and Solis-Perales (2008) is adopted in this work:

$$u = \frac{-1}{\beta_{\mathrm{E}}(\boldsymbol{z})}\left(z_{\rho+1} + \boldsymbol{K}^{\mathrm{T}}\boldsymbol{z}\right), \tag{7}$$

where $\boldsymbol{z} = [z_1, z_2, \cdots, z_\rho]$, the feedback gains $\boldsymbol{K}$ are designed such that all the roots of Hurwitz polynomial $P_{(\rho)}(s) = s^\rho + K_\rho s^{\rho-1} + \cdots + K_2 s + K_1 = 0$ lie in the left half complex plane, and $\beta_{\mathrm{E}}(\boldsymbol{z})$ is the estimate of $\beta(\boldsymbol{z}, \boldsymbol{\zeta})$ satisfying $\mathrm{sgn}(\beta_{\mathrm{E}}(\boldsymbol{z})) = \mathrm{sgn}(\beta(\boldsymbol{z}, \boldsymbol{\zeta}))$.

With such a feedback controller u, the stabilization of system (6) can be ensured and the proof is given in Lemma 2 in Appendix A. It is also remarked that the linear feedback controller (7) is a typical design for achieving chaos synchronization for many chaotic systems, including the Chen system, Lorenz systems, Lü system, Duffing oscillators, and Hindmarsh-Rose neuronal model. As these systems have been widely applied in practical applications (Femat *et al.*, 1999; Xu *et al.*, 2004; Haefner, 2005; Femat and Solis-Perales, 2008; Wang *et al.*, 2012), such as secure communication, system identification, physical systems, and biological systems, the proposed linear feedback control is desirable in practice.

As shown in Eq. (7), the control signal u is determined by the time derivatives of the observable state error, denoted as z_i. However, the exact values of z_i are unknown. To estimate them, some strategies have been developed, such as the linearizing feedback based estimator (Han, 1995; Femat *et al.*, 1999; Femat and Solis-Perales, 2008), and the nonlinear geometric based estimator (Li *et al.*, 2005). In this study, based on the methods proposed by Levant (2003) and Levant and Pavlov (2008), a high-order sliding mode based estimation strategy is proposed, which is more robust to system uncertainties owing to the adoption of sliding mode.

Theorem 2 Considering the master system (1), there exists a slave system (2) together with the linearizing feedback controller (7) and a high-order sliding mode based time differentiator estimator

$$\begin{cases} \dot{\hat{z}}_1 = \hat{z}_2 - L\lambda_1|\hat{z}_1 - z_1|^{\frac{\rho}{\rho+1}}\mathrm{sgn}(\hat{z}_1 - z_1), \\ \dot{\hat{z}}_i = \hat{z}_{i+1} - L^i\lambda_i|\hat{z}_1 - z_1|^{\frac{\rho-i+1}{\rho-i+2}}\mathrm{sgn}(\hat{z}_1 - z_1), \\ \dot{\hat{z}}_\rho = \hat{z}_{\rho+1} - L^\rho\lambda_\rho|\hat{z}_1 - z_1|^{\frac{1}{2}}\mathrm{sgn}(\hat{z}_1 - z_1) + \beta_{\mathrm{E}}(\hat{\boldsymbol{z}})u, \\ \dot{\hat{z}}_{\rho+1} = -L^{\rho+1}\lambda_{\rho+1}\mathrm{sgn}(\hat{z}_1 - z_1), \end{cases} \tag{8}$$

such that system (2) asymptotically synchronizes to system (1), where $1 < i < \rho$, $L > 0$ is the so-called high-gain parameter, interpreted as the uncertainties estimation rate and often chosen as a constant (Femat *et al.*, 2000; Yang and Shao, 2002), and λ_i and $\beta_{\mathrm{E}}(\hat{\boldsymbol{z}})$ are some positive constants.

Proof Subtracting system (1) from (2), we have the error dynamics (3). Then, the problem of synchronization is reduced to the stabilization of system (3). Based on Assumption 3 and Theorem 1, (3) can be further rearranged into a canonical form (6).

Let $\boldsymbol{\varpi} \in \mathbb{R}^{\rho+1}$ denote the vector of the estimation error and its components are defined as $\varpi_i = \hat{z}_i - z_i, i = 1, 2, \cdots, \rho + 1$. Subtracting the $(\rho+1)$th subsystem of (6a) from (8), we have

$$\begin{cases} \dot{\varpi}_1 = \varpi_2 - L\lambda_1|\varpi_1|^{\frac{\rho}{\rho+1}}\mathrm{sgn}(\varpi_1), \\ \dot{\varpi}_i = \varpi_{i+1} - L^i\lambda_i|\varpi_1|\dfrac{\rho-i+1}{\rho-i+2}\mathrm{sgn}(\varpi_1), \\ \qquad 2 \le i \le \rho - 1, \\ \dot{\varpi}_\rho = \varpi_{\rho+1} - L^\rho\lambda_\rho|\varpi_1|^{\frac{1}{2}}\mathrm{sgn}(\varpi_1), \\ \dot{\varpi}_{\rho+1} = -L^{\rho+1}\lambda_{\rho+1}\mathrm{sgn}(\varpi_1) - \Gamma(\boldsymbol{z}, z_{\rho+1}, \boldsymbol{\zeta}, u). \end{cases} \tag{9}$$

Define the following variables:

$$\begin{cases} v_1 = L^{\rho}|\varpi_1|^{\frac{\rho}{\rho+1}}\mathrm{sgn}(\varpi_1), \\ v_i = L^{\rho+1-i}|\varpi_1|^{\frac{\rho}{\rho+1}-\frac{\rho-i+1}{\rho-i+2}}\varpi_i, \ \ 2 \le i \le \rho, \\ v_{\rho+1} = \varpi_{\rho+1}. \end{cases} \quad (10)$$

Note that $\dot{v}_1 = L^{\rho}[|\varpi_1|^{\frac{\rho}{\rho+1}}\mathrm{sgn}(\varpi_1)]\dot{\varpi}_1$, where '$\cdot$' denotes the first derivative of time. Due to the boundedness of chaotic systems, z_1 is bounded. Therefore, to track the dynamics of z_1, $\hat{z}_1$ must be bounded too. Then, it can be derived that $[|\varpi_1|^{\frac{\rho}{\rho+1}-\frac{\rho-i+1}{\rho-i+2}}\mathrm{sgn}(\varpi_1)]$ is also bounded by a sufficiently large value, denoted as χ. Consequently, we have $\dot{v}_1 \le L^{\rho}\chi\dot{\varpi}_1$. Iteratively, we have the following 'estimating error system':

$$\dot{\overline{\boldsymbol{v}}} = L\boldsymbol{D}(\chi, \lambda_1, \ldots, \lambda_{\rho+1})\overline{\boldsymbol{v}} + \boldsymbol{\Omega}(\cdot), \quad (11)$$

where $\overline{\boldsymbol{v}} = (v_1, v_2, \cdots, v_{\rho+1})^{\mathrm{T}}$, $\boldsymbol{\Omega}(\cdot) = [0, 0, \cdots, -\Gamma]^{\mathrm{T}}$, and

$$\boldsymbol{D}(\chi, \lambda_1, \cdots, \lambda_{\rho+1}) = \begin{bmatrix} -\lambda_1\chi & \chi & 0 & \cdots & 0 \\ -\lambda_2 & 0 & 1 & \cdots & 0 \\ \vdots & \vdots & \vdots & & \vdots \\ -\lambda_{\rho} & 0 & 0 & \cdots & 1 \\ -\lambda_{\rho+1} & 0 & 0 & \cdots & 0 \end{bmatrix}.$$

According to Assumption 4, the time derivative $\dot{z}_{\rho}$ is bounded and thus $\Gamma(\cdot)$ is also bounded. By choosing suitable constants λ_i such that all the eigenvalues of $\boldsymbol{D}(\cdot)$ lie in the left-half complex plane, we have $v_i \to 0$, $1 \le i \le \rho+1$. That is to say, the estimating error system $\overline{\boldsymbol{v}}$ is globally asymptotically stable at zero, which implies $\varpi_i \to 0$, i.e., $\hat{z}_i \to z_i$ for $1 \le i \le \rho+1$. Consequently, the estimates of z_i can be duly obtained.

Then, by substituting $\hat{z}_i$ into the linearizing feedback control signal u in Eq. (7), we have the stabilization of error dynamics (6) based on Lemma 2 in Appendix A, i.e., $\boldsymbol{e} \to \boldsymbol{0}$, which implies that the synchronization between systems (1) and (2) can be achieved. The proof is completed.

Remark 5 Although the exact value of χ is unknown in practice, it can be estimated based on the prior information of the upper bound of the chaotic systems. The parameters λ_i's, as stated above, are selected such that all the eigenvalues of $\boldsymbol{D}(\cdot)$ lie in the left-half complex plane. Referring to Li *et al.* (2005) and Levant and Pavlov (2008), λ_i's are usually selected within $[1, 10]$. The high-gain parameter L is usually not very large, typically within $[5, 20]$ (Femat *et al.*, 2000; Yang and Shao, 2002).

Remark 6 Compared to the sliding mode methods given in Yang and Shao (2002) and Rodríguez *et al.* (2008) (see Types II and III in Appendix C), a simple linear combination of the state error and its time differentiator estimator is used and thus the computation of complicated controller u is avoided. It is also remarked that, although the proposed algorithm takes more computation than the algorithm proposed in Femat and Solis-Perales (2008) (see Type I in Appendix C), its synchronization performance can be significantly improved, owing to the combination of the sliding mode. This will be verified in the simulation section.

3 Numerical simulations

In this section, some simulation examples are presented to show the performance of the proposed robust synchronization strategy.

3.1 Example 1: synchronization of two Lorenz systems

The Lorenz system, which has been frequently studied in the context of chaos synchronization, is taken as our first example. It is a typical chaotic oscillator with its dynamics governed by the following equation:

$$\begin{cases} \dot{x}_{1\mathrm{m}} = p_1(x_{2\mathrm{m}} - x_{1\mathrm{m}}), \\ \dot{x}_{2\mathrm{m}} = p_2 x_{1\mathrm{m}} - x_{2\mathrm{m}} - x_{1\mathrm{m}}x_{3\mathrm{m}}, \\ \dot{x}_{3\mathrm{m}} = x_{1\mathrm{m}}x_{2\mathrm{m}} - p_3 x_{3\mathrm{m}}. \end{cases} \quad (12)$$

Then, the slave system can be constructed as

$$\begin{cases} \dot{x}_{1\mathrm{s}} = q_1(x_{2\mathrm{s}} - x_{1\mathrm{s}}) + \beta_{\mathrm{E}}(\hat{\boldsymbol{z}})u, \\ \dot{x}_{2\mathrm{s}} = q_2 x_{1\mathrm{s}} - x_{2\mathrm{s}} - x_{1\mathrm{s}}x_{3\mathrm{s}}, \\ \dot{x}_{3\mathrm{s}} = x_{1\mathrm{s}}x_{2\mathrm{s}} - q_3 x_{3\mathrm{s}}. \end{cases} \quad (13)$$

Let $z_i = e_i = x_{i\mathrm{s}} - x_{i\mathrm{m}}$. Subtracting system (12) from (13), we have the error dynamics

$$\begin{cases} \dot{e}_1 = \Delta f_1 + \beta_{\mathrm{E}}(\hat{\boldsymbol{z}})u, \\ \dot{e}_2 = \Delta f_2, \\ \dot{e}_3 = \Delta f_3, \end{cases} \quad (14)$$

where Δf_i denotes the uncertainties between the master and the slave. Based on Theorem 1, system (14) can be changed into the following canonical

form:

$$\begin{cases} \dot{z}_1 = z_2 + \beta_{\mathrm{E}}(\hat{\boldsymbol{z}})u, \\ \dot{z}_2 = \Gamma(z_1, z_2, \boldsymbol{\zeta}, u), \\ \dot{\boldsymbol{\zeta}} = \Psi(z_1, \boldsymbol{\zeta}), \end{cases} \tag{15}$$

where $\beta_{\mathrm{E}}(\hat{\boldsymbol{z}})$ is generally selected as a constant, and $\boldsymbol{\zeta} = (e_2, e_3)$.

Following the design given in Section 2, a robust synchronization scheme based on a combination of high-order sliding mode and linearizing feedback control can be designed as follows:

$$\begin{cases} \dot{\hat{z}}_1 = \hat{z}_2 - L\lambda_1|\hat{z}_1 - z_1|^{\frac{1}{2}}\mathrm{sgn}(\hat{z}_1 - z_1) + \beta_{\mathrm{E}}(\hat{\boldsymbol{z}})u, \\ \dot{\hat{z}}_2 = -L^2\lambda_2\mathrm{sgn}(\hat{z}_1 - z_1), \\ u = \dfrac{-1}{\beta_{\mathrm{E}}(\hat{\boldsymbol{z}})}\left(\hat{z}_2 + K_1\hat{z}_1\right). \end{cases} \tag{16}$$

Using the controller (16) and according to Theorem 2, we have $z_i \to 0$. Then, it is concluded that the error dynamics (15) asymptotically converges to zero, as the subsystem $\Psi(0, \boldsymbol{\zeta})$ is a minimum-phase system (The proof is shown in Appendix B).

In the simulation, the initial conditions are randomly selected from $[0, 1]$ and the initial estimates are set as zeros, i.e., $\hat{z}_1 = \hat{z}_2 = 0$. The true parameter values are $p_1 = 10$, $p_2 = 28$, $p_3 = 8/3$, while the auxiliary parameter values are $q_1 = 9.5$, $q_2 = 26.6$, $q_3 = 2.533$, and $q_1 = 9.0$, $q_2 = 25.2$, $q_3 = 2.4$, corresponding to 5% and 10% of parameter mismatches, respectively. $\beta_{\mathrm{E}}(\hat{z})$ is set as 20, and the other constants are chosen as $\chi = 4$, $L = 20$, $\lambda_1 = 1$, $\lambda_2 = 5$, and $K_1 = 10$. The control signal is activated at $t = 2$ s. For comparison, the simulation results with different designs proposed in Yang and Shao (2002), Femat and Solis-Perales (2008), and Rodríguez *et al.* (2008) are also demonstrated, which are named Types I, II, and III, respectively, while our proposed design is referred to as Type IV. The designs of Types I, II, and III are listed in Appendix C.

Fig. 1 depicts the synchronization error between the master and the slave for different approaches. Note that our proposed scheme shows the strongest robustness and the fastest convergence among these four schemes. Such peculiarities are reasoned by the insensitivity of the high-order sliding mode to the system uncertainties and the simplicity of linear feedback control. The performances of Types I and II are similar, while Type III shows the worst performance. The reason is that Type III uses a sign-form control signal, which is a discrete-time control function. Therefore, a high control energy and a large oscillation are experienced due to the switching phenomenon of the control surface.

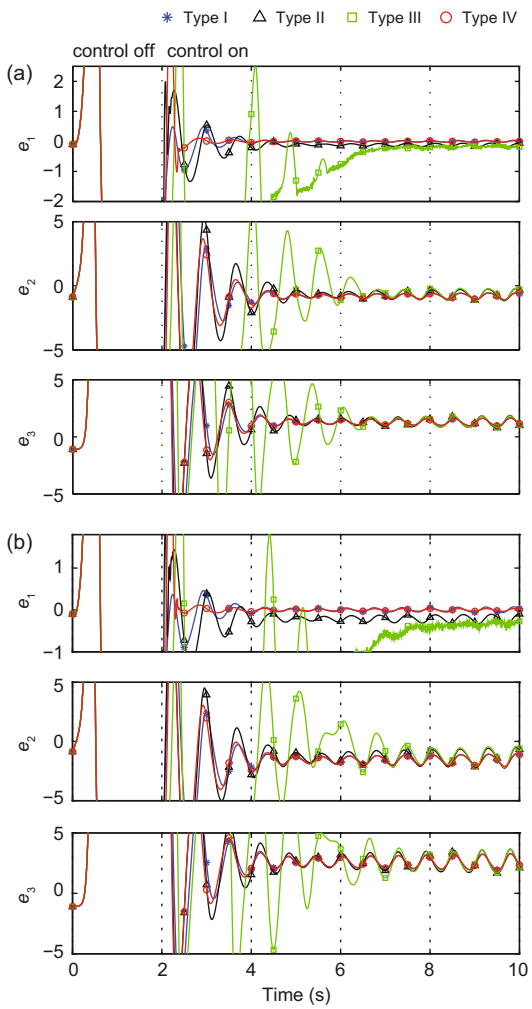

Fig. 1 The synchronization errors between the master and the slave of different methods with 5% (a) and 10% (b) of parameter mismatches. References to color refer to the online version of this figure

Note that the controller u is not equal to zero even when the synchronization between the master and the slave is established, since the controller must pay the cost of the synchronization with dynamic compensation.

3.2 Example 2: synchronization of Duffing and van der Pol oscillators

In the second example, the synchronization of two systems with different structures is considered. The master is the Duffing system expressed as

follows:

$$\begin{cases} \dot{x}_{1\mathrm{m}} = x_{2\mathrm{m}}, \\ \dot{x}_{2\mathrm{m}} = x_{1\mathrm{m}} - p_1 x_{2\mathrm{m}} - x_{1\mathrm{m}}^3 + p_2 \cos(\omega_{\mathrm{m}} t), \end{cases} \tag{17}$$

where $x_{1\mathrm{m}}$ is measured.

The slave system is a van der Pol oscillator with its dynamics governed by

$$\begin{cases} \dot{x}_{1\mathrm{s}} = x_{2\mathrm{s}}, \\ \dot{x}_{2\mathrm{s}} = q_1(1 - x_{1\mathrm{s}}^2)x_{2\mathrm{s}} - x_{1\mathrm{s}}^3 + q_2 \cos(\omega_{\mathrm{s}} t) + \beta_{\mathrm{E}}(\hat{\boldsymbol{z}})u. \end{cases} \tag{18}$$

Subtracting system (17) from (18), we have the following error dynamics:

$$\begin{cases} \dot{e}_1 = e_2, \\ \dot{e}_2 = \Delta f + \beta_{\mathrm{E}}(\hat{\boldsymbol{z}})u, \end{cases} \tag{19}$$

where $\Delta f = x_{1\mathrm{m}} - p_1 x_{2\mathrm{m}} - x_{1\mathrm{m}}^3 + p_2 \cos(\omega_{\mathrm{m}} t) - [q_1(1 - x_{1\mathrm{s}}^2)x_{2\mathrm{s}} - x_{1\mathrm{s}}^3 + q_2 \cos(\omega_{\mathrm{s}} t)]$ denotes the uncertainty between the master and the slave.

To achieve the synchronization between systems (17) and (18), a robust control strategy can be designed as follows:

$$\begin{cases} \dot{\hat{z}}_1 = \hat{z}_2 - L\lambda_1 |\hat{z}_1 - z_1|^{2/3} \mathrm{sgn}(\hat{z}_1 - z_1), \\ \dot{\hat{z}}_2 = \hat{z}_3 - L^2 \lambda_2 |\hat{z}_1 - z_1|^{1/2} \mathrm{sgn}(\hat{z}_1 - z_1) + \beta_{\mathrm{E}}(\hat{\boldsymbol{z}})u, \\ \dot{\hat{z}}_3 = -L^3 \lambda_3 \mathrm{sgn}(\hat{z}_1 - z_1), \\ u = \dfrac{-1}{\beta_{\mathrm{E}}(\hat{\boldsymbol{z}})} \left(\hat{z}_3 + K_2 \hat{z}_2 + K_1 \hat{z}_1\right). \end{cases} \tag{20}$$

In the simulation, the initial states of the master and the slave are randomly selected from $[0, 1]$, while the initial values of $\hat{z}_i$ are set as zeros. It is letting $p_1 = 0.15$, $p_2 = 1.75$, $\omega_{\mathrm{m}} = 0.5$ for the master, while $q_1 = 0.1$, $q_2 = 1.0$, $\omega_{\mathrm{s}} = 1.0$ and $\beta_{\mathrm{E}}(\hat{\boldsymbol{z}}) = 1$ for the slave. The other parameters are set as $\chi = 10$, $L = 10$, $\lambda_1 = 2$, $\lambda_2 = 3$, $\lambda_3 = 4$. The feedback gains are set as $K_1 = K_2 = 50$ such that the characteristic polynomial equation $P_{(\rho)}(s) = s^2 + K_2 s + K_1 = 0$ is Hurwitz. The control signal is activated at $t = 10$ s.

The synchronization errors between Duffing and van der Pol oscillators are shown in Fig. 2. It is observed that, the robust synchronization between the slave system (18) and the master system (17) can be established in general, although their structures are totally different. As shown in Fig. 2, Type III is still inferior to the others due to the same reason mentioned in Section 3.1. However, benefitting from the design of the recursive linearizing feedback control law, our proposed Type IV design can significantly

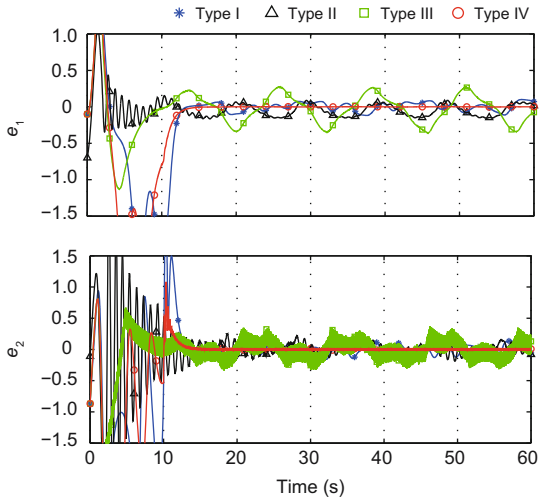

Fig. 2 The synchronization errors between Duffing and van der Pol oscillators with different methods. References to color refer to the online version of this figure

reduce the high frequency oscillation and hence outperform the others from the viewpoints of accuracy and convergence rate. These numerical simulations suggest that our proposed Type IV design is more robust to both parametric and structural mismatches. Therefore, it is recommended and used as the sole design in the following simulations.

3.3 Synchronization of biological neuronal networks

Synchronization plays an important role in information processing for large ensembles of neurons (Wang *et al.*, 2000; Mao, 2009). Therefore, understanding the mechanism underlying synchronization is more meaningful in neuroscience and thus has been receiving more and more attention in the last two decades. As we all know, human brain is composed of a large number of neurons. On one hand, it is very difficult, if not impossible, to get all the information of a whole neuronal network. On the other hand, we are usually interested in a small portion of neurons. Therefore, it is unrealistic and uneconomic to measure all the state information of a biological neuronal network. Instead, the synchronization of a sub-network is more preferable and is thus studied for this example.

The diagram of the considered biological neuronal network is depicted in Fig. 3. The whole network can be regarded as two sub-networks connected via neurons 1 and 7. Since synchronization typically

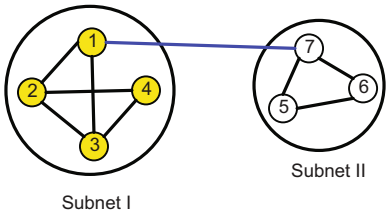

Fig. 3 The diagram of a biological neuronal network

exists between different biological oscillators, it is assumed that neurons in subnets I and II are modeled by the Hindmarsh-Rose model and FitzHugh-Nagumo model, respectively, which are expressed in the following.

Subnet I:

$$\begin{cases} \dot{x}_{i\mathrm{m}} = p_{i1}x_{i\mathrm{m}}^2 - x_{i\mathrm{m}}^3 - y_{i\mathrm{m}} - w_{i\mathrm{m}} \\ \qquad\quad + c\sum_{j=1}^{7} H_{ij}(x_{j\mathrm{m}} - x_{i\mathrm{m}}), \\ \dot{y}_{i\mathrm{m}} = (p_{i1} + p_{i2})x_{i\mathrm{m}}^2 - y_{i\mathrm{m}}, \\ \dot{w}_{i\mathrm{m}} = p_{i3}(p_{i4}x_{i\mathrm{m}} + p_{i5} - w_{i\mathrm{m}}), \\ \qquad i = 1, 2, 3, 4, \end{cases} \tag{21}$$

where $x_{i\mathrm{m}}$ is the membrane potential, and $y_{i\mathrm{m}}$ and $w_{i\mathrm{m}}$ are the recovery variables with respect to the fast and slow currents, respectively. The last term in the first equation of Eq. (21) indicates the coupling between the ith neuron and the others in the network, where c is the coupling coefficient, and $\boldsymbol{H}$ is the connection matrix of the system, where $H_{ij} = 1$ if neurons i and j are connected, and $H_{ij} = 0$ otherwise. It is also assumed that $H_{ij} = H_{ji}$ and $H_{ii} = -\sum_{j=1,i\neq j}^{7} H_{ij}$.

Subnet II:

$$\begin{cases} \dot{x}_{i\mathrm{m}} = p_{i6}(y_{i\mathrm{m}} + x_{i\mathrm{m}} - \dfrac{x_{i\mathrm{m}}^3}{3} + 3\gamma) \\ \qquad\quad + c\sum_{j=1}^{7} H_{ij}(x_{j\mathrm{m}} - x_{i\mathrm{m}}), \\ \dot{y}_{i\mathrm{m}} = -(x_{i\mathrm{m}} - p_{i7} + p_{i8}y_{i\mathrm{m}})/3, \quad i = 5, 6, 7, \end{cases} \tag{22}$$

where $1 - 2p_{i8}/3 < p_{i7} < 1$, $0 < p_{i8} < 1$, $p_{i8} < p_{i6}^2$, $\gamma = -0.4$ is the stimulus intensity, $x_{i\mathrm{m}}$ shares the properties of both membrane potential and excitability, and $y_{i\mathrm{m}}$ is responsible for accommodation. Similar to subnet I, the last term in the first equation of Eq. (22) denotes the coupling effect with the same definition as Eq. (21).

We focus on the dynamics of subnet I. Assuming that only the states of subnet I are measurable, a subsystem for subnet I is constructed such that the trajectories of neurons 1–4 are tracked. Since only the membrane potential of the electrical biological model can be easily measured in the experiment, it is assumed that only $x_{i\mathrm{m}}, i = 1, 2, 3, 4$ are measurable, and the other system states are assumed to be unknown. Following the design proposed in Section 2, the slave system can be designed as

$$\begin{cases} \dot{x}_{i\mathrm{s}} = q_{i1}x_{i\mathrm{s}}^2 - x_{i\mathrm{s}}^3 - y_{i\mathrm{s}} - w_{i\mathrm{s}} + c\sum_{j=1}^{7} H_{ij}(x_{j\mathrm{s}} - x_{i\mathrm{s}}) \\ \qquad\quad + \beta_{\mathrm{E}}(\hat{\boldsymbol{z}})u_i, \\ \dot{y}_{i\mathrm{s}} = (q_{i1} + q_{i2})x_{i\mathrm{s}}^2 - y_{i\mathrm{s}}, \\ \dot{w}_{i\mathrm{s}} = q_{i3}(q_{i4}x_{i\mathrm{s}} + q_{i5} - w_{i\mathrm{s}}), \ i = 1, 2, 3, 4, \end{cases} \tag{23}$$

together with a robust control strategy

$$\begin{cases} \dot{\hat{z}}_{i1} = \hat{z}_{i2} - L\lambda_1|\hat{z}_{i1} - z_{i1}|^{1/2}\mathrm{sgn}(\hat{z}_{i1} - z_{i1}) + \beta_{\mathrm{E}}(\hat{\boldsymbol{z}})u_i, \\ \dot{\hat{z}}_{i2} = -L^2\lambda_2\mathrm{sgn}(\hat{z}_{i1} - z_{i1}), \\ u_i = \dfrac{-1}{\beta_{\mathrm{E}}(\hat{\boldsymbol{z}})}\big(\hat{z}_{i2} + K_1\hat{z}_{i1}\big), \end{cases} \tag{24}$$

where $z_{i1} = x_{i\mathrm{s}} - x_{i\mathrm{m}}$. Since the Hindmarsh-Rose model is a minimum-phase system, based on Theorem 2, it can be easily concluded that the states of the slave (23) converge to those of the master (21).

In the simulation, we set the coupling coefficient $c = 0.1$. Parameters p_{ij}'s of subnet I are randomly selected within 5% of reference values $p_{i1}^0 = 2.8$, $p_{i2}^0 = 1.6$, $p_{i3}^0 = 0.001$, $p_{i4}^0 = 9$, $p_{i5}^0 = 5$, $p_{i6}^0 = 3$, $p_{i7}^0 = 0.7$, $p_{i8}^0 = 0.8$, and the parameters of the slave system q_{ij} are uniformly set as the reference ones, i.e., $q_{ij} = p_{ij}^0$. The other parameters are set as $\chi = 5$, $L = 10$, $\lambda_1 = 1$, $\lambda_2 = 5$, $K_1 = 10$, $\beta_{\mathrm{E}}(\hat{\boldsymbol{z}}) = 10$, and the control signal is switched on at $t = 10$ s.

The simulation results are given in Fig. 4. Note that a long time is needed for achieving synchronization of the third state, as it evolves slowly compared to the variables of the other two states. Therefore, the simulation results for the third state variable are omitted here, and only the synchronization errors of the first and second state variables are given. Figs. 4a and 4b show that although the exact structure of the whole network is unknown, a computational model can be constructed by combining the high-order sliding mode based information reconstruction technique with linear feedback control, such that the trajectory of the original neuronal network can be well tracked. This indicates that the

proposed robust scheme provides a useful and physically realizable method to achieve synchronization of biological neuronal networks.

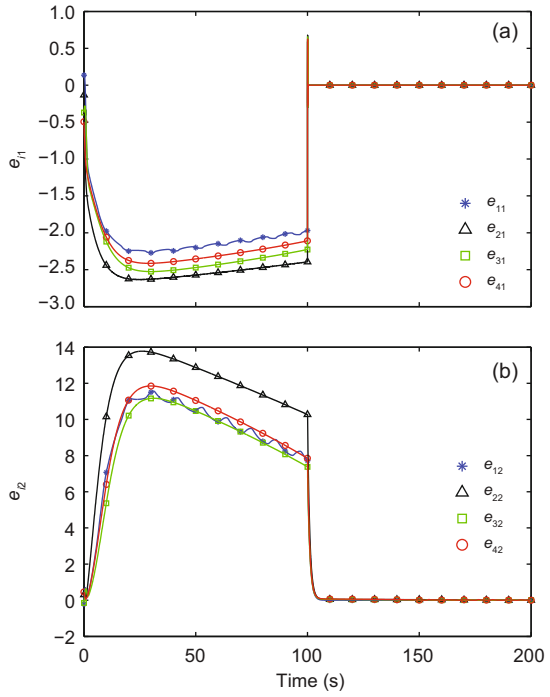

Fig. 4 Synchronization errors e_{i1} (a) and e_{i2} (b) ($i = 1, 2, 3, 4$) of subnet I. References to color refer to the online version of this figure

4 Conclusions

In this paper, a robust synchronization approach has been proposed, in which a high-order sliding mode observer is proposed to estimate the synchronization error and its time derivatives, while a feedback control law constructed by a linear function of the estimated time differentiator is used to drive the dynamics of the slave to follow that of the master. The feasibility of the proposed design has been verified and some examples have been simulated. Simulation results show that the proposed algorithm can achieve the synchronization of chaotic systems even if there are some modeling and parametric mismatches. Note that although this work considers only the case that only one system state is observable, it provides a promising approach to achieving synchronization of some practical systems like real circuits. Some more complicated cases, for example, a combination of the system state variables is measurable, will be studied in the near future.

References

Besancon, G., 2000. Remarks on nonlinear adaptive observer design. *Syst. Contr. Lett.*, **41**(4):271-280. [doi:10.1016/S0167-6911(00)00065-7]

Bowong, S., 2004. Stability analysis for the synchronization of chaotic systems with different order: application to secure communications. *Phys. Lett. A*, **326**(1-2):102-113. [doi:10.1016/j.physleta.2004.04.004]

Chen, M., Kurths, J., 2007. Chaos synchronization and parameter estimation from a scalar output signal. *Phys. Rev. E*, **76**(2):027203. [doi:10.1103/PhysRevE.76.027203]

Collins, J.J., Stewart, I.N., 1993. Coupled nonlinear oscillators and the symmetries of animal gaits. *J. Nonl. Sci.*, **3**(1):349-392. [doi:10.1007/BF02429870]

Feki, M., 2003. An adaptive chaos synchronization scheme applied to secure communication. *Chaos Sol. Fract.*, **18**(1):141-148. [doi:10.1016/S0960-0779(02)00585-4]

Femat, R., Solis-Perales, G., 2008. Robust Synchronization of Chaotic Systems via Feedback. Springer. [doi:10.1007/978-3-540-69307-9]

Femat, R., Alvarez-Ramírez, J., Castillo-Toledo, B., *et al.*, 1999. On robust chaos suppression in a class of nonlinear oscillators: application to Chua's circuit. *IEEE Trans. Circ. Syst. I*, **46**(9):1150-1152. [doi:10.1109/81.788818]

Femat, R., Alvarez-Ramírez, J., Fernández-Anaya, G., 2000. Adaptive synchronization of high-order chaotic systems: a feedback with low-order parametrization. *Phys. D*, **139**(3-4):231-246. [doi:10.1016/S0167-2789(99)00226-2]

Femat, R., Ortiz, R.J., Perales, G.S., 2001. An adaptive chaos synchronization scheme applied to secure communication scheme via robust asymptotic feedback. *IEEE Trans. Circ. Syst. I*, **48**(10):1161-1169.

Freitas, U.S., Macau, E.E.N., Grebogi, C., 2005. Using geometric control and chaotic synchronization to estimate an unknown model parameter. *Phys. Rev. E*, **71**(4):047203. [doi:10.1103/PhysRevE.71.047203]

Grassi, G., Mascoio, S., 1999. Synchronizing hyperchaotic systems by observer design. *IEEE Trans. Circ. Syst. II*, **46**(4):478-483. [doi:10.1109/82.755422]

Haefner, J.W., 2005. Modeling Biological Systems: Principles and Applications. Springer, New York, USA.

Han, J.Q., 1995. The extended state observer of a class of uncertain systems. *Contr. & Dec.*, **110**(1):85-88 (in Chinese).

Isidori, A, 1989. Nonlinear Control System. Springer-Verlag, Berlin, Germany.

Karimi, H.R., 2011. Robust synchronization and fault detection of uncertain master-slave systems with mixed time-varying delays and nonlinear perturbations. *Int. J. Contr. Automat. Syst.*, **9**(4):671-680. [doi:10.1007/s12555-011-0408-8]

Karimi, H.R., 2012. A sliding mode approach to H_∞ synchronization of master-slave time-delay systems with Markovian jumping parameters and nonlinear uncertainties. *J. Franklin Inst.*, **349**(4):1480-1496. [doi:10.1016/j.jfranklin.2011.09.015]

Karimi, H.R., Gao, H., 2010. New delay-dependent exponential H_∞ synchronization for uncertain neural networks with mixed time-delays. *IEEE Trans. Syst. Man Cybern. Part B*, **40**(1):173-185. [doi:10.1109/TSMCB.2009.2024408]

Kocarev, L., Parlitz, U., 1995. General approach for chaotic synchronization with applications to communication. *Phys. Rev. Lett.*, **74**(25):5028-5031. [doi:10.1103/PhysRevLett.74.5028]

Levant, A., 2003. Higher-order sliding modes, differentiation and output-feedback control. *Int. J. Contr.*, **76**(9-10):924-941. [doi:10.1080/0020717031000099029]

Levant, A., Pavlov, Y., 2008. Generalized homogeneous quasi-continuous controllers. *Int. J. Robust Nonl. Contr.*, **18**(4-5):385-398. [doi:10.1002/rnc.1199]

Li, X.R., Zhao, L.Y., Zhao, G.Z., 2005. Sliding mode control for synchronization of chaotic systems with structure or parameter mismatching. *J. Zhejiang Univ.-Sci.*, **6**(6):571-576. [doi:10.1631/jzus.2005.A0571]

Liu, Y., Tang, W., 2009. Adaptive synchronization of chaotic systems and its uses in cryptanalysis. *In*: Recent Advances in Nonlinear Dynamics and Synchronization (NDS-1), Theory and Applications. Springer, **254**:307-346.

Liu, Y., Tang, W., Kocarev, L., 2008. An adaptive observer design for the auto-synchronization of Lorenz system. *Int. J. Bifurcat. Chaos*, **18**(8):2415-2423. [doi:10.1142/S0218127408021786]

Mao, Y., 2009. Adaptive Synchronization and Its Use in Biological Neural Network Modeling. MS Thesis, City University of Hong Kong, Hong Kong, China.

Mao, Y., Tang, W., Liu, Y., *et al.*, 2009. Identification of biological neurons using adaptive observers. *Cogn. Process.*, **10**(Suppl 1):41-53. [doi:10.1007/s10339-008-0230-2]

Nijmeijer, H., Mareels, I.M.Y., 1997. An observer looks at synchronization. *IEEE Trans. Circ. Syst. I*, **44**(10):882-890. [doi:10.1109/81.633877]

Pecora, L.M., Carroll, T.L., 1990. Synchronization in chaotic systems. *Phys. Rev. Lett.*, **64**(8):821-824.

Pecora, L.M., Carroll, T.L., 1991. Driving systems with chaotic signals. *Phys. Rev. A*, **44**(4):2374-2383. [doi:10.1103/PhysRevA.44.2374]

Rodríguez, A., de León, J., Fridman, L., 2008. Quasi-continuous high-order sliding-mode controllers for reduced-order chaos synchronization. *Int. J. Nonl. Mech.*, **43**(9):948-961. [doi:10.1016/j.ijnonlinmec.2008.07.007]

Trentelman, H.L., Takaba, K., Monshizadeh, N., 2013. Robust synchronization of uncertain linear multi-agent systems. *IEEE Trans. Automat. Contr.*, **58**(6):1511-1523. [doi:10.1109/TAC.2013.2239011]

Wang, B., Shi, P., Karimi, H.R., *et al.*, 2012. H_∞ robust controller design for the synchronization of master-slave chaotic systems with disturbance input. *Model. Identif. Contr.*, **33**(1):27-34. [doi:10.4173/mic.2012.1.3]

Wang, Y., Chik, D.T.M., Wang, Z.D., 2000. Coherence resonance and noise-induced synchronization in globally coupled Hodgkin-Huxley neurons. *Phys. Rev. E*, **61**(1):740-746. [doi:10.1103/PhysRevE.61.740]

Wittmeier, S., Song, G., Duffin, J., *et al.*, 2008. Pacemakers handshake synchronization mechanism of mammalian respiratory rhythmogenesis. *PNAS*, **105**(46):18000-18005. [doi:10.1073/pnas.0809377105]

Xu, J., Min, L., Chen, G., 2004. A chaotic communication scheme based on generalized synchronization and hash functions. *Chin. Phys. Lett.*, **21**(8):1445-1448. [doi:10.1088/0256-307X/21/8/009]

Yang, T., Shao, H.H., 2002. Synchronizing chaotic dynamics with uncertainties based on a sliding mode control design. *Phys. Rev. E*, **65**(4):046210. [doi:10.1103/PhysRevE.65.046210]

Youssef, T., Chadli, M., Karimi, H.R., *et al.*, 2013. Chaos synchronization based on unknown input proportional multiple-integral fuzzy observer. *Abstr. Appl. Anal.*, **2013**:670878. [doi:10.1155/2013/670878]

Yu, D., Parlitz, U., 2008. Estimating parameters by autosynchronization with dynamics restrictions. *Phys. Rev. E*, **77**(6 Pt 2):066221. [doi:10.1103/PhysRevE.77.066221]

Appendix A: Lemmas

Lemma 1 (Femat *et al.*, 2001) Let us assume that there exists a coordinate transformation $\boldsymbol{z}=\boldsymbol{\Phi}(\boldsymbol{x})$ such that the following nonlinear system

$$\begin{cases}\dot{\boldsymbol{x}}=f(\boldsymbol{x})+g(\boldsymbol{x})u,\\ y=h(\boldsymbol{x}),\end{cases}\tag{A1}$$

can be transformed into the following canonical form:

$$\begin{cases}\dot{z}_i=z_{i+1},\ i=1,2,\cdots,\rho-1,\\ \dot{z}_\rho=\alpha(\boldsymbol{z},\boldsymbol{\zeta})+\beta(\boldsymbol{z},\boldsymbol{\zeta})u,\ \beta(\boldsymbol{z},\boldsymbol{\zeta})\neq 0,\end{cases}\tag{A2a}$$

$$\begin{cases}\dot{\boldsymbol{\zeta}}=\Psi(\boldsymbol{z},\boldsymbol{\zeta}),\ \ \boldsymbol{\zeta}\in\mathbb{R}^{n-\rho},\\ y=z_1.\end{cases}\tag{A2b}$$

Now suppose there is an estimate $\beta_{\mathrm{E}}(\boldsymbol{z})$, defined by the Lie derivative along an uncertain function $\beta(\boldsymbol{z},\boldsymbol{\zeta})=L_gL_f^{\rho-1}h(\boldsymbol{x})\neq 0$, such that $\mathrm{sgn}(\beta_{\mathrm{E}}(\boldsymbol{z}))=\mathrm{sgn}(\beta(\boldsymbol{z},\boldsymbol{\zeta}))$. Define $\delta(\boldsymbol{z},\boldsymbol{\zeta})=\beta(\boldsymbol{z},\boldsymbol{\zeta})-\beta_{\mathrm{E}}(\boldsymbol{z})$, $\Theta(\boldsymbol{z},\boldsymbol{\zeta},u)=\alpha(\boldsymbol{z},\boldsymbol{\zeta})+\delta(\boldsymbol{z},\boldsymbol{\zeta})u$, and $z_{\rho+1}=\Theta(\boldsymbol{z},\boldsymbol{\zeta},u)$. Then, there exists an invariant manifold such that the nonlinear system (A2) can be rewritten in the following form:

$$\begin{cases}\dot{z}_i=z_{i+1},\ i=1,2,\cdots,\rho-1,\\ \dot{z}_\rho=z_{\rho+1}+\beta_{\mathrm{E}}(\boldsymbol{z})u,\\ \dot{z}_{\rho+1}=\Gamma(\boldsymbol{z},z_{\rho+1},\boldsymbol{\zeta},u),\end{cases}\tag{A3a}$$

$$\begin{cases}\dot{\boldsymbol{\zeta}}=\Psi(\boldsymbol{z},\boldsymbol{\zeta}),\\ y=z_1,\end{cases}\tag{A3b}$$

where $\Gamma(\boldsymbol{z},z_{\rho+1},\boldsymbol{\zeta},u)=\sum_{i=1}^{\rho-1}[z_{i+1}\partial_i\Theta(\boldsymbol{z},\boldsymbol{\zeta},u)]+\delta(\boldsymbol{z},\boldsymbol{\zeta})\dot{u}+\partial_t\delta(\boldsymbol{z},\boldsymbol{\zeta})u+[z_{\rho+1}+\beta_{\mathrm{E}}(\boldsymbol{z})]\partial_\rho\Theta(\boldsymbol{z},\boldsymbol{\zeta},u)+\partial_\zeta\Theta(\boldsymbol{z},\boldsymbol{\zeta},u)\Psi(\boldsymbol{z},\boldsymbol{\zeta})$, and $\partial_i\Theta(\boldsymbol{z},\boldsymbol{\zeta},u)=\partial\Theta(\boldsymbol{z},\boldsymbol{\zeta},u)/\partial x_i$.

Proof By definition, we have $\delta(\boldsymbol{z},\boldsymbol{\zeta})=\beta(\boldsymbol{z},\boldsymbol{\zeta})-\beta_{\mathrm{E}}(\boldsymbol{z})$, $\Theta(\boldsymbol{z},\boldsymbol{\zeta},u)=\alpha(\boldsymbol{z},\boldsymbol{\zeta})+\delta(\boldsymbol{z},\boldsymbol{\zeta})u$, and $z_{\rho+1}=\Theta(\boldsymbol{z},\boldsymbol{\zeta},u)$. Under the trajectories of the system (A3), we have a manifold $\Xi(\boldsymbol{z},z_{\rho+1},\boldsymbol{\zeta},u)=$

$z_{\rho+1} - \Theta(\boldsymbol{z},\boldsymbol{\zeta},u)$ and $\mathrm{d}\Xi(\boldsymbol{z},z_{\rho+1},\boldsymbol{\zeta},u)/\mathrm{d}t = 0$ (i.e., it is a time invariant manifold with boundary) for the initial condition $\Xi_0 = 0$. By definition, $\Xi(\boldsymbol{z},z_{\rho+1},\boldsymbol{\zeta},u) = z_{\rho+1} - \Theta(\boldsymbol{z},\boldsymbol{\zeta},u)$ and $\mathrm{d}\Xi(\boldsymbol{z},z_{\rho+1},\boldsymbol{\zeta},u)/\mathrm{d}t = 0$, which means that $\Xi(\boldsymbol{z},z_{\rho+1},\boldsymbol{\zeta},u)$ is the first integral of the nonlinear system (A2). Therefore, the solution of system (A3) is a projection of the solution of system (A2). Since system (A2) is a transformation of the uncertain nonlinear system (A1), system (A3) is also dynamically equivalent to system (A1).

Lemma 2 (Femat *et al.*, 2001) Let the state-feedback control be $u = \frac{-1}{\beta_{\mathrm{E}}(\boldsymbol{z})}\left(z_{\rho+1} + \boldsymbol{K}^{\mathrm{T}}\boldsymbol{z}\right)$, where the feedback gains $\boldsymbol{K}$ are coefficients of the Hurwitz polynomial $P_{(\rho)}(s) = s^{\rho}+K_1 s^{\rho-1}+\cdots+K_{\rho-1}s+K_{\rho}$. Then, the solution of $(\boldsymbol{z}(t),z_{\rho+1}(t),\boldsymbol{\zeta}(t))$ in system (A3) converges to the origin if the subsystem $\dot{\boldsymbol{\zeta}} = \Psi(\boldsymbol{z},\boldsymbol{\zeta})$ in (A3) is a minimum-phase system and the initial condition satisfies $\Xi_0 = 0$.

Proof It is supposed that the initial conditions satisfy $\Xi_0 = 0$. Since $\Xi(\boldsymbol{z},z_{\rho+1},\boldsymbol{\zeta},u)$ is an invariant manifold, we have $z_{\rho+1} = \Theta(\boldsymbol{z},\boldsymbol{\zeta},u)$ for all $t \geq 0$. Then, we have $z_{\rho+1} = \alpha(\boldsymbol{z},\boldsymbol{\zeta}) + \delta(\boldsymbol{z},\boldsymbol{\zeta})u$, where $\delta(\boldsymbol{z},\boldsymbol{\zeta}) = \beta(\boldsymbol{z},\boldsymbol{\zeta}) - \beta_{\mathrm{E}}(\boldsymbol{z})$. Combining $z_{\rho+1}$ with the state feedback controller, we have $u = \frac{-1}{\beta(\boldsymbol{z},\boldsymbol{\zeta})}[\alpha(\boldsymbol{z},\boldsymbol{\zeta})+\boldsymbol{K}^{\mathrm{T}}\boldsymbol{z}]$. Since $\alpha(\boldsymbol{z},\boldsymbol{\zeta})$ is also a smooth function of its arguments, the augmented state $z_{\rho+1}(t)$ and the state feedback controller $u = u(\boldsymbol{z})$ are bounded. On the other hand, the convergence of the states $(\boldsymbol{z}(t),z_{\rho+1}(t))$ follows from the fact that the subsystem (A3a) is in cascade form and the corresponding characteristic polynomial is Hurwitz under a state feedback controller. In addition, if $(\boldsymbol{z}(t),z_{\rho+1}(t)) = 0$, the subsystem $\dot{\boldsymbol{\zeta}} = \Psi(0,\boldsymbol{\zeta})$ converges to the origin as it is a minimum-phase system. Therefore, the state feedback is a practical stabilizer for system (A3).

Appendix B: Internal stability of the synchronization error dynamics of two Lorenz systems

Let us consider two Lorenz systems, where the master system is expressed as follows:

$$\begin{cases} \dot{x}_{1\mathrm{m}} = p_1(x_{2\mathrm{m}} - x_{1\mathrm{m}}), \\ \dot{x}_{2\mathrm{m}} = p_2 x_{1\mathrm{m}} - x_{2\mathrm{m}} - x_{1\mathrm{m}}x_{3\mathrm{m}}, \\ \dot{x}_{3\mathrm{m}} = x_{1\mathrm{m}}x_{2\mathrm{m}} - p_3 x_{3\mathrm{m}}, \end{cases} \tag{B1}$$

and the slave system is

$$\begin{cases} \dot{x}_{1\mathrm{s}} = p_1(x_{2\mathrm{s}} - x_{1\mathrm{s}}) + u, \\ \dot{x}_{2\mathrm{s}} = p_2 x_{1\mathrm{s}} - x_{2\mathrm{s}} - x_{1\mathrm{s}}x_{3\mathrm{s}}, \\ \dot{x}_{3\mathrm{s}} = x_{1\mathrm{s}}x_{2\mathrm{s}} - p_3 x_{3\mathrm{s}}. \end{cases} \tag{B2}$$

Let $z_1 = e_1 = x_{1\mathrm{s}} - x_{1\mathrm{m}}$ be the only observable state error. Based on Lemma 1, the error dynamics can be changed into a canonical form as follows:

$$\begin{cases} \dot{z}_1 = \Gamma(\cdot) + u, \\ \dot{\xi}_1 = p_2 z_1 - \xi_1 - z_1\xi_2, \\ \dot{\xi}_2 = z_1\xi_1 - p_3\xi_2, \\ y = z_1, \end{cases} \tag{B3}$$

where $z_1 = e_1$, $\boldsymbol{\xi} = (\xi_1,\xi_2)^{\mathrm{T}} = (e_2,e_3)^{\mathrm{T}}$, $\rho = 1$. So, we have the following subsystem:

$$\dot{\boldsymbol{\xi}} = \boldsymbol{A}\boldsymbol{\xi} + \boldsymbol{B}S, \tag{B4}$$

where $\boldsymbol{A} = \begin{bmatrix} -1 & -z_1 \\ z_1 & -p_3 \end{bmatrix}$, $\boldsymbol{B} = \begin{bmatrix} p_2 \\ 0 \end{bmatrix}$, and $S = z_1$.

For the Lorenz system, the polynomial $P(s) = \lambda^2 + (p_3+1)\lambda + (p_3 + z_1^2)$ is Hurwitz; i.e., the eigenvalues of matrix $\boldsymbol{A}$ lie in the left-half complex plane. As the states of the Lorenz system are bounded in a circle, the state error z_1 is also bounded. Hence, system $\Psi(0,\boldsymbol{\zeta})$ is asymptotically stable; consequently, (B1) is a minimum-phase system.

Note that due to the characteristics of chaotic attractors, we can draw the same conclusion for the other chaotic systems, like Chua's system and the Hindmarsh-Rose neuronal model.

Appendix C: Design of other robust synchronization schemes

Type I: linearizing feedback control scheme

Referring to Femat and Solis-Perales (2008), the Type I observer is designed as

$$\begin{cases} \dot{\hat{z}}_i = \hat{z}_{i+1} - L^i k_i(\hat{z}_1 - z_1), \ i = 1,2,\cdots,\rho-1, \\ \dot{\hat{z}}_{\rho} = \hat{z}_{\rho+1} - L^{\rho}k_{\rho}(\hat{z}_1 - z_1) + \beta_{\mathrm{E}}(\hat{\boldsymbol{z}})u, \\ \dot{\hat{z}}_{\rho+1} = -L^{\rho+1}k_{\rho+1}(\hat{z}_1 - z_1), \\ u = \dfrac{-1}{\beta_{\mathrm{E}}(\hat{\boldsymbol{z}})}\left(\hat{z}_{\rho+1} + \boldsymbol{K}^{\mathrm{T}}\hat{\boldsymbol{z}}\right), \end{cases} \tag{C1}$$

where $\hat{z}_i$ is the estimate of its corresponding state z_i and $z_1 = e_1$. The coefficients k_i and K_i are chosen

such that their corresponding characteristics of polynomial, i.e., $P_{(\rho+1)}(s)=s^{\rho+1}+k_1s^{\rho}+\cdots+k_{\rho}s+k_{\rho+1}=0$ and $P_{(\rho)}(s)=s^{\rho}+K_1s^{\rho-1}+\cdots+K_{\rho-1}s+K_{\rho}=0$, are Hurwitz. L is a high-gain estimation parameter.

Type II: Yang's sliding mode observer

Referring to Yang and Shao (2002), the Type II observer is designed as

$$\begin{cases}\dot{\hat{z}}_1=\hat{z}_2-L\lambda_1|\hat{z}_1-z_1|^{\frac{1}{2}}\mathrm{sgn}(\hat{z}_1-z_1),\\ \dot{\hat{z}}_i=\hat{z}_{i+1}-L^i\lambda_i|\hat{z}_1-z_1|^{\frac{1}{2}}\mathrm{sgn}(\hat{z}_1-z_1),\ 2\le i\le\rho,\\ \dot{\hat{z}}_{\rho+1}=-L^{\rho+1}\lambda_{\rho+1}|\hat{z}_1-z_1|^{\frac{1}{2}}\mathrm{sgn}(\hat{z}_1-z_1),\\ S=\hat{z}_{\rho+1}+\displaystyle\int_0^t\left[\sum_{j=1}^{\rho}c_j\hat{z}_j+c_{\rho+1}(\hat{z}_{\rho+1}+u)\right]\mathrm{d}t,\\ u=\displaystyle\int_0^t\left\{\alpha S-\beta\mathrm{sgn}(S)-\dot{\hat{z}}_{\rho+1}\right.\\ \qquad\left.-\left[\sum_{j=1}^{\rho}c_j\hat{z}_j+c_{\rho+1}(\hat{z}_{\rho+1}+u)\right]\right\}\mathrm{d}t,\end{cases}\tag{C2}$$

where $0<\alpha<1,\beta>0$.

Type III: high-order sliding mode observer

Referring to Rodríguez *et al.* (2008), the Type III observer is designed as

$$\begin{cases}\dot{\hat{z}}_1=v_1,\\ v_1=\hat{z}_2-\lambda_1|\hat{z}_1-z_1|^{\frac{\rho}{\rho+1}}\mathrm{sgn}(\hat{z}_1-z_1),\\ \dot{\hat{z}}_i=v_i,\ 2\le i\le\rho-1,\\ v_i=\hat{z}_{i+1}-\lambda_i|\hat{z}_i-v_{i-1}|^{\frac{\rho-i+1}{\rho-i+2}}\mathrm{sgn}(\hat{z}_i-v_{i-1}),\\ \qquad 2\le i\le\rho-1,\\ \dot{\hat{z}}_{\rho}=v_{\rho},\\ v_{\rho}=\hat{z}_{\rho+1}-\lambda_{\rho}|\hat{z}_{\rho}-v_{\rho-1}|^{\frac{1}{2}}\mathrm{sgn}(\hat{z}_{\rho}-v_{\rho-1}),\\ \dot{\hat{z}}_{\rho+1}=-\lambda_{\rho+1}\mathrm{sgn}(\hat{z}_{\rho+1}-v_{\rho}),\end{cases}\tag{C3}$$

where u is a quasi-continuous controller designed as follows:

$$\begin{cases}\varphi_{0,\rho}=e_1,\quad N_{0,\rho}=|e_1|,\\ \Psi_{0,\rho}=\dfrac{\varphi_{0,\rho}}{N_{0,\rho}}=\mathrm{sgn}(e_1),\\ \varphi_{i,\rho}=e_1^{(i)}+\gamma_iN_{i=1,\rho}^{\frac{\rho-i}{\rho-i+1}}\Psi_{i-1,\rho},\\ N_{i,\rho}=|e_1^{(i)}|+\gamma_iN_{i-1,\rho}^{\frac{\rho-i}{\rho-i+1}},\\ \Psi_{i,\rho}=\dfrac{\varphi_{i,\rho}}{N_{i,\rho}}.\end{cases}$$